4282 *Chem. Mater.* **2009,** *21,* 4282–4287
DOI:10.1021/cm901472x

CHEMISTRY OF MATERIALS
Article

A Novel Approach for the Fabrication of Silica and Silica/Metal Hybrid Microtubes

Kamlesh Kumar,*,† Bhanu Nandan,† Valeriy Luchnikov,‡ Frank Simon,† Anastasia Vyalikh,† Ulrich Scheler,† and Manfred Stamm*,†

†*Leibniz Institute of Polymer Research Dresden, Hohe Strasse 6, 01069 Dresden, Germany, and* ‡*Insitut de Sciences des Matériaux de Mulhouse, IS2M, LRC 7228, CNRS, 15 rue Jean Starcky, BP 2488, 68057 Mulhouse Cedex, France*

Received May 29, 2009. Revised Manuscript Received August 5, 2009

This paper describes a novel and simple method to fabricate silica and silica/metal hybrid microtubes of very high aspect ratio via self-rolling of polymer layers. A trilayer of poly(dimethylsiloxane) (PDMS)/polystyrene (PS)/poly(4-vinylpyridine) (P4 VP) self-rolled into microtubes, when exposed to a solvent selective for P4 VP chains, because of the strain generated by the swelling of P4 VP layer. Oxidative pyrolysis of the polymer tubes at 700 °C removes all the organic part of the tube and converts PDMS into silica. Moreover, by depositing a metallic layer on the tripolymer layer, it was possible to obtain silica/metal hybrid tubes. The metallic layer can form the inner or outer wall of the tube by depositing it over or under the PDMS layer. The fabricated tubes were further characterized by optical microscopy, Fourier transform infrared (FTIR), high-resolution scanning electron microscopy (HRSEM), X-ray photoelectron spectroscopy (XPS), energy-dispersive analysis (EDX), ^{29}Si solid-state nuclear magnetic resonance (^{29}Si NMR), and focused ion beam (FIB). The silica and silica/metal hybrid tubes have potential applications in micro- and nanofluidic devices, optoelectronic devices, and in catalysis.

1. Introduction

Recently, various structures of silicon dioxide have been used in biological, medical, and biotechnological applications.[1−3] The properties of silica, especially its high thermal and chemical stability, photoluminescency, biocompatibility, and high strength, lead to many applications such as in nano and microelectronics, optoelectronics, waveguide, and transport media for medical applications.[4−7] Apart from silica tubes, in recent years, silica/metal hybrid mesostructures have attracted much interest because of the combination of their different properties. Hybrid silica/metal composites are expected to have many advantages and possible applications in medicine, physics, and chemistry. For the catalytic applications, composites of silica with metals such as gold, titanium, platinum, aluminum, etc., have been synthesized.[8−10]

In the past, a number of methods such as template-based method,[11] laser ablation,[12,13] thermal oxidation,[14] and chemical vapor deposition[15,16] have been reported to fabricate silica tubes and wires. The major limiting factor in these approaches is the problem of attaining high aspect ratio. In this paper, we report a simple, novel, and inexpensive robust preceramic procedure to fabricate silica tubes of high aspect ratio. Preceramic polymers have been widely used to synthesize ceramic film via thermal curing and pyrolysis.[17] Here, we used poly(dimethylsiloxane) (PDMS) as a precursor of silica. PDMS is widely used as a precursor for the silica layer, and the surface of PDMS can be converted to silicon

*Corresponding author. E-mail: kksaini@gmail.com (K.K.); stamm@ipfdd.de (M.S.). Tel: +493514658632. Fax: +49-3514658281.

(1) Feng, J.; Yan, W.; Gou, Z.; Weng, W.; Yang, D. *J. Mater. Sci.: Mater. Med.* **2007**, *18*, 2167.
(2) Barik, T. K.; Sahu, B.; Swain, V. *Parasitol. Res.* **2008**, *103*(2), 253.
(3) Coradin, T.; Nassif, N.; Livage, J. *Appl. Microbiol. Biotechnol.* **2003**, *61*(5), 429.
(4) Pavesi, L.Lockwood, D. J. *Silicon Photonics*; Topics in Applied Physics; Springer: Berlin, 2004; Vol. *94*, p 177.
(5) Soref, R. A. *Proc. IEEE* **1993**, *81*(12), 1687.
(6) Songmuang, R.; Rastelli, A.; Mendach, S.; Denke, Ch.; Schmidt, O. G. *Microelectron. Eng.* **2007**, *84*, 1427.
(7) McAllister, D. V.; Cros, F.; Davis, S. P.; Matta, L. M.; Prausnitz, M. R.; Allen, A. G. *Proceedings of the 10th International Conference on Solid-State Sensors and Actuators* (*Transducers'99*)*, Technical Digest*; Sendai, Japan, June 7−10, 1999; IEEE: Piscataway, NJ, 1999; p 1098.
(8) Kim, Y. H.; Lee, D. K.; Cha, H. G.; Kim, C. W.; Kang, Y. C.; Kang, Y. S. *J. Phys. Chem. B* **2006**, *110*, 24923.
(9) Fang, C. L.; Qian, K.; Zhu, J.; Wang, S.; Lv, X.; Yu, S. H. *Nanotechnology* **2008**, *19*, 125601.
(10) Liu, N. G.; Prall, B. S.; Klimov, V. I. *J. Am. Chem. Soc.* **2006**, *128*, 15362.
(11) Li, N.; Li, X.; Wang, W.; Qiu, S. *Mater. Chem. Phys.* **2005**, *91*, 223.
(12) Yu, D. P.; Hung, Q. L.; Ding, Y.; Zhang, H. Z.; Bai, Z. G.; Wang, J. J.; Zhou, Y. H.; Qian, W.; Xiong, G. C.; Feng, S. Q. *Appl. Phys. Lett.* **1998**, *73*, 3076.
(13) Chaudhary, Y. S.; Ghatak, J.; Bhatta, U. M.; Khushalani, D. *J. Mater. Chem.* **2006**, *16*, 3619.
(14) Hu, J. Q.; Jiang, Y.; Meng, X. M.; Lee, C. S.; Lee, S. T. *Chem. Phys. Lett.* **2003**, *367*, 339.
(15) Wu, X. C.; Song, W. H.; Wang, K. Y.; Hu, T.; Zhao, B.; Sun, Y. P.; Du, J. J. *Chem. Phys. Lett.* **2001**, *336*, 53.
(16) Niu, J.; Sha, J.; Zhang, N.; Ji, Y.; Ma, X.; Yang, D. *Physica E* **2004**, *23*, 1.
(17) Seyferth, D. *Adv. Chem. Ser.* **1990**, *224*, 565.

Published on Web 08/21/2009

oxide by various techniques such as low-temperature plasma oxidation,[18] UV/ozone treatment,[19−21] and pyrolytic degradation.[22,23]

Recently, different three-dimensional structures of semiconductor, metal, and polymer have been fabricated using strain-driven self-rolling technique.[24−30] The strain in the film can arise by unequal thermal expansion of top and bottom layer,[31] different crystal lattice constants of top and bottom layer,[26−29] or unequal swelling of film in selective solvent.[24,25] The mechanism of rolling-up of the polymer bifilms is very general and the strain is generated because of the different degree of swelling of the constituting polymer layers. Polystyrene (PS) and poly(4-vinylpyridine) (P4 VP) constitute a good choice of the materials of the bilayer. PS demonstrates minimal water uptake thus forming a stiff hydrophobic film upon exposure to water. P4 VP is less hydrophobic and swells in acidic aqueous solutions because of protonation of polymer chains. The strained film, when allowed to relax, releases strain and tries to attain minimum potential energy by scrolling. The rolling of the layers results in the formation of the tubes. Hence, by adopting such an approach, micro and nanotubes were fabricated by self-rolling of thin bilayer polymer films (PS/P4 VP) gradually released from a solid substrate.[24,30] The dimension of the tubes was found to be affected by a number of parameters and has been discussed elsewhere.[32] Recently, metal and bimetallic tubes were also fabricated using the self-rolled polymer tubes as sacrificial template.[33]

In this work, we adopted the self-rolling phenomena of polymer layers to produce silica and silica/metal hybrid tube. A thin film of PDMS was rolled with the P4 VP/PS bilayer resulting in the formation of PDMS/P4 VP/PS trilayer polymer tube. These polymer tubes were then pyrolyzed in an oxidative environment that converted PDMS into silica and simulatenously removed the organic part of the tube. Furthermore, it will be shown that by depositing a thin film of metal along with the PDMS layer, it is possible to fabricate silica/metal hybrid tubes. The main advantage of this approach is the possibility of the formation of ceramic tubes of very high aspect ratio using a preceramic procedure. Furthermore, silica can be combined with any metal or combination of metals for fabricating silica/metal hybrid tubes.

2. Experimental Section

Materials. PDMS (Sylgard 184 silicone elastomer kit) was obtained from Dow Corning. The PDMS solution consisted of a mixture of base and its curing agent in a ratio 10:1 and was degassed in a vacuum oven before making the solution in diethylether. P4 VP (M_n = 45900 g/mol, M_w = 82500 g/mol) and PS (M_n = 600 000 g/mol, M_w = 654 000 g/mol) were purchased from Polymer Source Inc. Dodecylbenzenesulfonic acid (DBSA), diethyl ether, chloroform, and toluene were obtained from Aldrich. All chemicals were used without any further purification.

Fabrication of PDMS/PS/P4 VP Tube. A bilayer of PS and P4 VP was deposited on the cleaned silicon wafer from toluene and chloroform solution, respectively. The thickness of PS was 60 nm and P4 VP thickness was 80 nm for all samples. Dip-coater was used to deposit the films on the substrate. The bilayer was cross-linked by UV radiation emitted through a UV lamp (G8T5, TecWest Inc., USA). UV lamp had a particular 2.5W output at 254 nm. The samples were exposed for 20 min and estimated exposure dose for 20 min was 2.74 J/cm^2. A 200 nm thick layer of PDMS was deposited from the diethyl ether solution, on the cross-linked bilayer. The PDMS layer was thermally cross-linked at 120 °C for 2 h. Microstructuring of the cross-linked layers was done by a sharp blade to introduce a selective solvent in the bottom layer. The rolling of microstructure sample was done in an 4 wt % aqueous DBSA solution.

Fabrication of PDMS/PS/P4 VP/Au Tube. A thin layer of gold (4−6 nm) was deposited on the cross-linked polymer layers for fabricating the hybrid tubes. The gold layer was deposited by sputter coater (Balzers SCD 050). Three different kind of hybrid tubes were fabricated by depositing gold (a) before the PDMS layer deposition, (b) after the PDMS layer deposition, (c) before and after the PDMS layer.

Fabrication of Silica and Silica/Au Tube. The polymer tubes after being rolled in the DBSA solution were dried in the air and then pyrolyzed at 700 °C for 4 h in oxygen atmosphere and allowed to cool down to room temperature. The pyrolysis process removed the organic components in the tube and transformed the PDMS layer into silica layer.

Characterization Techniques. The morphology and chemical composition of the tubes were characterized by optical microscopy, HRSEM, FTIR, EDX, XPS, and FIB. HRSEM was performed using a Zeiss Ultra 55 Gemini scanning electron microscope with an acceleration voltage of 5 kV. FTIR spectrum of the tube was obtained by FTIR spectrometer IFS 66v/s [Bruker, Germany]. The spectrum were recorded in the transmission mode for the sample on silicon wafer. The FTIR spectrum of the sample was obtained after subtraction of the neat silicon wafer spectra. Axis Ultra (Kratos Analytical, England) spectrometer with Mono-Al Kα X-ray source of 300 W at 20 mA was used to record the XPS spectra of tubes. The maximum information depth of the XPS method is not more than 8−10 nm. EDX of the samples was carried out in a Philips XL30 scanning electron microscope. The openings in the tubes were demonstrated using the FIB (Zeiss NEON 40 EsB). The FIB system works at high vacuum (1.69×10^{-6} mbar). In

(18) Fateh-Alavi, K.; Gedde, U. W. *Polym. Degrad. Stab.* **2004**, *84*(3), 469.
(19) Schnyder, B.; Lippert, T.; Kötz, R.; Wokaun, A.; graubner, V. M.; Nuyken, O. *Surf. Sci.* **2003**, *532*, 1067.
(20) Egitto, F. D.; Matienzo, L. J. *J. Mater. Sci.* **2006**, *41*, 6362.
(21) Park, H. B.; Han, D. W.; Lee, Y. M. *Chem. Mater.* **2003**, *15*(12), 2346.
(22) Nakade, M.; Ichihashi, K.; Ogawa, M. *J. Ceram. Soc. Jpn.* **2005**, *113*(4), 280.
(23) Nakade, M.; Ichihashi, K.; Ogawa, M. *J. Porous Mater.* **2005**, *12*, 79.
(24) Luchnikov, V.; Sydorenko, O.; Stamm, M. *Adv. Mater.* **2005**, *17*, 1177.
(25) Luchnikov, V.; Kumar, K.; Stamm, M. *J. Micromech. Microeng.* **2008**, *18*, 35041.
(26) Nastauschev, Y. V.; Prinz, V. Y.; Svitasheva, S. N. *Nanotechnology* **2005**, *16*, 908.
(27) Schmidt, O. G.; Eberl, K. *Nature* **2001**, *410*, 6825.
(28) Deneke, C.; Muller, C.; Jin-Phillipp, N. Y.; Schmidt, O. G. *Semicond. Sci. Technol.* **2002**, *17*, 1278.
(29) Songmuang, R.; Denke, C. H.; Schmidt, O. G. *Appl. Phys. Lett.* **2006**, *89*, 223109.
(30) Luchnikov, V.; Stamm, M. *Physica E* **2007**, *37*, 236.
(31) Timoshenko, S. *J. Opt. Soc. Am.* **1925**, *11*, 233.
(32) Kumar, K.; Luchnikov, V.; Nandan, B.; Senkovskyy, V.; Stamm, M. *Eur. Polym. J.* **2008**, *44*(22), 4115.
(33) Kumar, K.; Nandan, B.; Luchnikov, V.; Gowd, E. B.; Stamm, M. *Langmuir* **2009**, *25*(13), 7667.

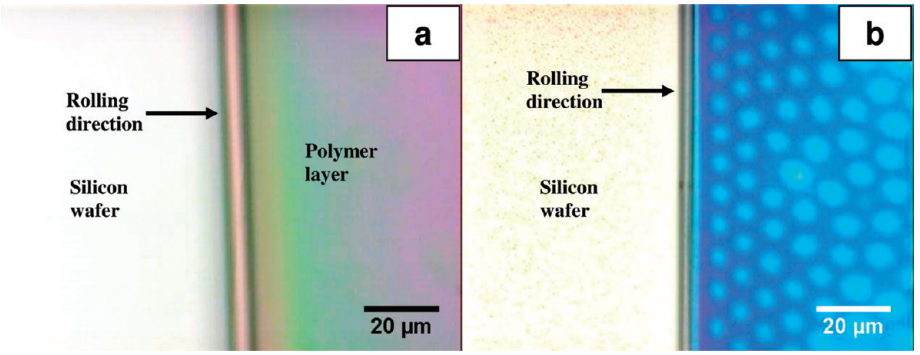

Figure 1. Optical micrographs of tube (a) before pyrolysis, (b) after pyrolysis.

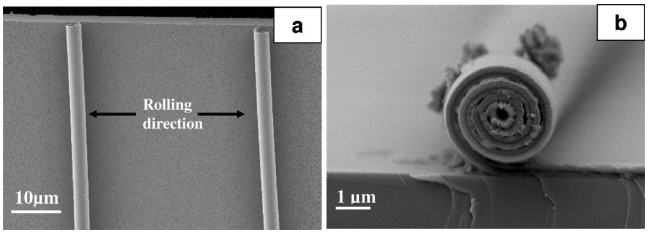

Figure 2. SEM micrographs of PDMS/PS/P4 VPpolymer tube before pyrolysis. (a) Tubes rolled in opposite direction from the scratch, (b) clearly visible rolled polymer layers with open end of tube.

FIB technique the samples were irradiated by 30 keV Ga^+ ions at 500 pA ion current. ^{29}Si solid-state NMR of the unpyrolyzed and pyrolyzed samples were acquired on a Bruker Avance 500 NMR spectrometer operating at a resonance frequency of 99.36 MHz for ^{29}Si using a Bruker BL3.2 MAS probe-head accepting 3.2-mm o.d. zirconium rotors with a sample spinning speed of 10 kHz. Single-pulse spectra have been recorded under high-power ^1H decoupling with an excitation pulse duration of 4 μs and a recycle delay of 40 s. To reference ^{29}Si chemical shifts Q8M8 was used as an external standard, which gives a $Si(-CH_3)_3$ signal at 12.6 ppm relative TMS.

3. Results and Discussion

The formation of the silica and silica/metal hybrid tubes consisted of a two-step procedure. In the first step, PDMS/PS/P4 VP tube was fabricated; it was then further subjected to pyrolysis in the second step to remove the polymer moiety. An optical micrograph of self- rolled polymer (PDMS/PS/P4 VP) tube before and after pyrolysis are shown in Figure 1. The direction of rolling is from left to right in both samples. It was observed that large density change occurs during the pyrolysis. This densification led to 40−50% volumetric shrinkage of the tube. However, the cylindrical shape of the tube was retained in the course of pyrolysis. The diameter of the tubes before and after pyrolysis were 7.1 and 3.3 μm, respectively.

The morphologies of pyrolyzed and unpyrolyzed tubes were further characterized in detail by HRSEM. Figure 2 shows the SEM images of polymer tube before pyrolysis. Figure 2a shows the rolling direction of polymer layer from a scratch. It is obvious that polymer layers roll in opposite directions from the scratch. The cross-section of the rolled polymer layer is shown in Figure 2b. The PS/P4 VP and PDMS layer can be distinguished in this image.

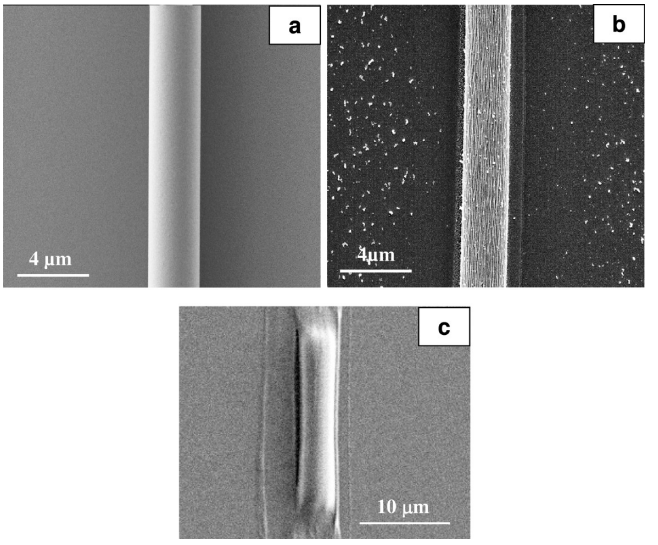

Figure 3. SEM micrographs of tube: (a) before pyrolysis, (b) after pyrolysis, (c) after annealing 1 h at 1200 °C.

The polymer layer completed three rolls before the rolling was stopped by taking the sample out from the acidic solution.

The morphology of tube's surface changed significantly after pyrolysis as shown in Figure 3. The as-rolled polymer tube surface was observed to be quite smooth (Figure 3 a) whereas after the pyrolysis wrinkles were formed on the tube surface making it exteremly rough (Figure 3b). Remarkably enough, the wrinkles on the pyrolyzed tube were oriented parallel to the tube's axis. These wrinkles can be eliminated by annealing of the tubes via heating them over 1000 °C for some time. In our preliminary experiments, the wrinkles were annealed at 1200 °C for 1 h (Figure 3c). However, this treatment leads also to partial collapse of the tubes. More detailed study is needed to determine the optimal temperature regime of the wrinkles annealing.

The roughness of the tube surface should be due to the inhomogeneous shrinkage of the structure. PDMS shrinks during the pyrolysis process but the tubular shape is maintained. The diameter of tubes was found to be smaller than the unpyrolyzed reference tube. Therefore, it was obvious that thermal decomposition of the polymer tube was accompanied by the creation of the exterior rough surface and partial mass removal from the polymer

tube. This mass loss was due to the removal of organic components during the pyrolysis.

The fabricated tube have hollow interior throughout the length of tube. The open end of fabricated tubes was confirmed by SEM as shown by images a and b in Figure 4. The usual approach for obtaining the tube's cross-sections is simply breaking the silicon wafer substrate. However, breaking of the substrate does not provide the tube's opening at exact position. The tube's opening can be obtained with high spatial resolution by using FIB cutting. The exact positioning of the tubes on the substrate and their opening at well-defined locations is important for the construction of future tube-based devices. Figure 5a shows two openings of a silica tube, one opening created by breaking of substrate (mark no. 1) and the other (mark no. 2) produced by FIB technique. A magnified image of the marked rectangular part of Figure 5a confirms almost perfect cylindrical shape of the object (Figure 5b). It is worth being mentioned here that except for the image of the tube presented in Figure 5, the opening in all other tubes shown elsewhere in this paper were imaged simply by breaking the silicon wafer.

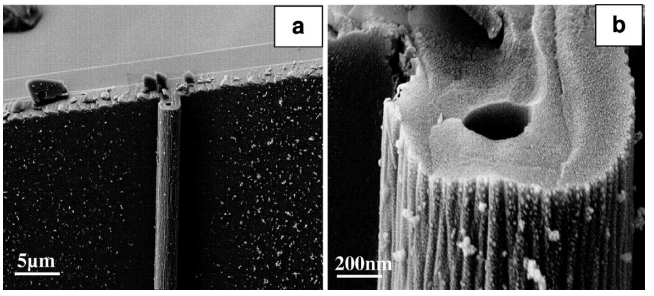

Figure 4. SEM micrographs of silica tube with open end (a) at lower magnification (b) at higher magnification.

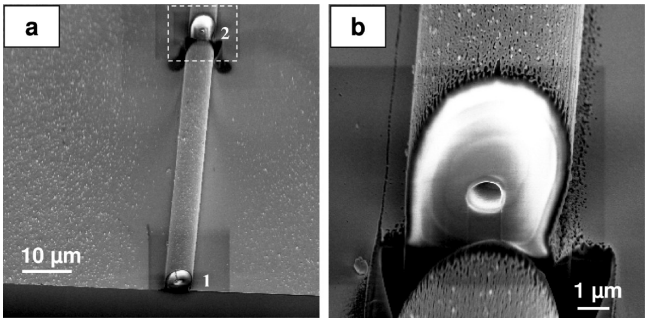

Figure 5. (a) Open end of silica tube by FIB (mark no. 2) as well as by breaking of silicon wafer (mark no. 1), (b) enlarged image of marked part of the Figure a.

The tube left after the pyrolysis process was entirely composed of silica because it is well-known that PDMS transforms into silica during the oxidative pyrolysis process. The reaction proceeds by decomposition of the PDMS producing amorphous SiO_2.[34] Scheme 1 shows the detailed reaction sequence:

The transformation of PDMS to silica was confirmed by FTIR analysis of the tube before and after pyrolysis. Figure 6 shows the spectra of pyrolyzed and unpyrolyzed sample. The characteristic peak of Si-CH_3 appeared at (1416, 1257, 804 cm^{-1}) and stretching vibration of CH_3 and CH_2 bond are observed at 2959 and 2929 cm^{-1} in unpyrolyzed samples. These characteristic peaks of Si-CH_3, CH_3, and CH_2 disappeared after pyrolysis at 700 °C. The characteristic peaks of Si−O asymmetric stretching vibration in PDMS appeared at 1091 and 1026 cm^{-1}. These peaks shifted to a higher wavenumber

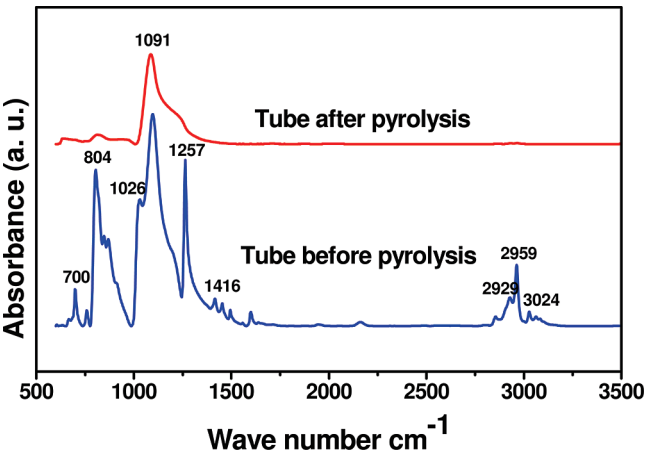

Figure 6. FTIR spectrum of PDMS/PS/P4 VP tube, before pyrolysis and after pyrolysis.

Scheme 1. Transformation of PDMS into Silica by Oxidative Pyrolysis

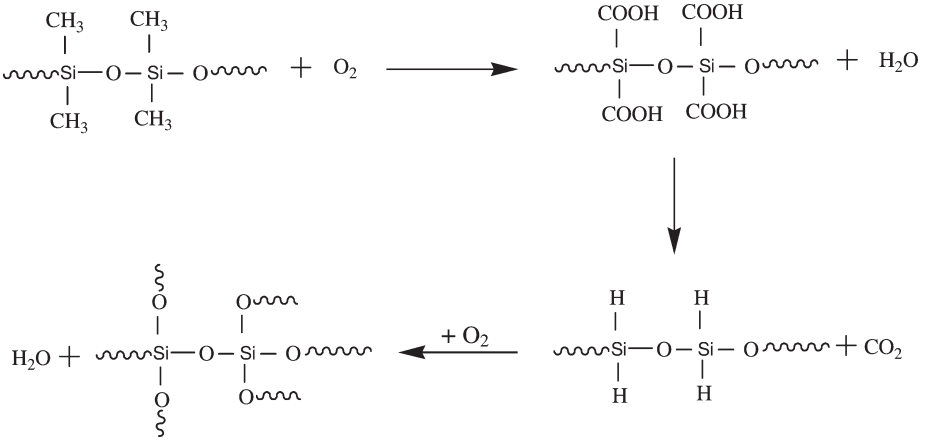

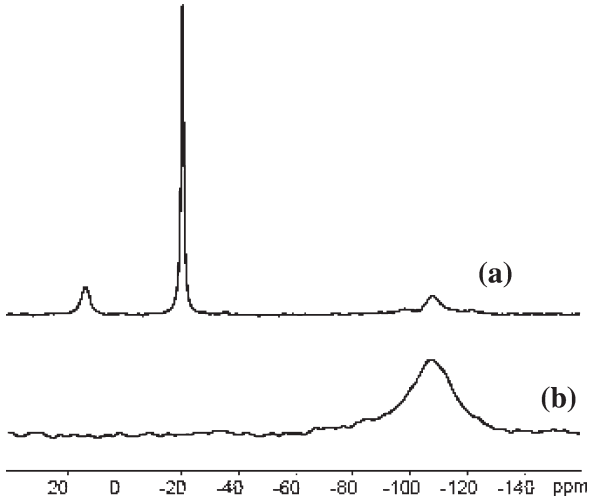

Figure 7. ^{29}Si MAS NMR spectrum of the PDMS (a) before pyrolysis and (b) after pyrolysis.

region after heat treatment. The shifting of Si−O to higher frequency is due to thermal transformation of PDMS to silica and formation of a strong Si−O bond. These shifting in frequency are related to change in bonding characteristic, such as bond length and bond angle.

Furthermore, the transformation of PDMS to silica was also investigated by ^{29}Si MAS NMR spectroscopy. The ^{29}Si MAS NMR spectra of the unpyrolyzed and pyrolyzed sample were shown in Figure 7. In unpyrolyzed sample spectrum, two intense and sharp signals at −21.2 ppm and 12.3 ppm arise from Si-CH_3 groups within the siloxane chain and at the chain ends, respectively, and are characteristic of linear PDMS. The group of the signals between −96.0 and −123.4 ppm and a minor peak at −36.8 ppm are attributed to other components (curing agents, etc.) composing the commercial silicone elastomer used in this study. In the pyrolzed sample, a single broadened signal centered at −107.9 ppm covers a range of chemical shifts characteristic of silica network, which extend from −92 ppm for oxygen-bridged Si with two geminal OH groups to −109 ppm for a networked silicon site bound to four SiO moieties. Therefore, we attribute the spectrum of the pyrolyzed sample to silica. Disappearance of characteristic PDMS peaks at −21.2 and 12.3 ppm in the spectrum of the pyrolyzed sample clearly indicates complete transformation of PDMS to silica.

Next, we discuss the fabrication of the silica/metal hybrid tubes. Using the present self-rolling technique, it was possible to fabricate any silica tubes in combination with any metal. In the present study, we demonstrated the formation of silica/gold hybrid tube. A 4−6 nm thin layer of gold was deposited before or after the deposition of PDMS layer. A polymer moiety was removed by oxidative pyrolysis resulting in the formation of silica/gold tube. Figure 8 hows the SEM micrographs of the hybrid tube after the heat treatment. The presence of silica and gold layer is clearly visible in the hybrid tubes. The

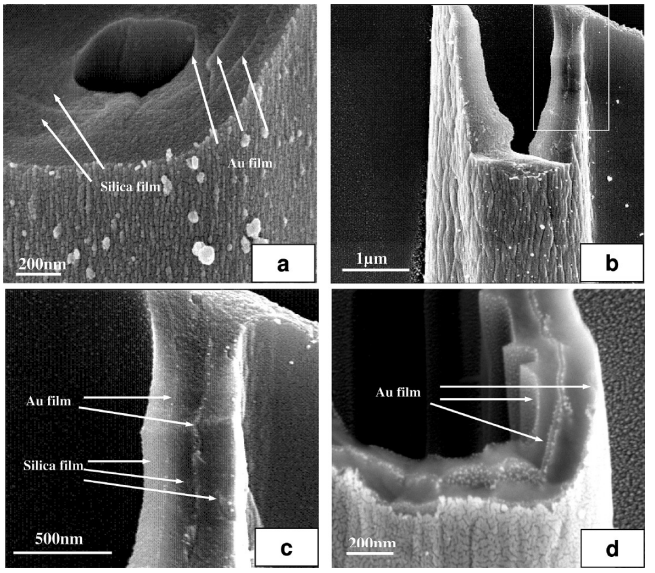

Figure 8. SEM images of silica/gold hybrid tubes: (a) gold layer is deposited on the top of thermally cross-linked PDMS layer; (b) gold film is deposited before depositon of the PDMS layer; (c) magnified image of the rectangular part of b; (d) gold films deposited before and after the PDMS layer.

thickness of gold layer (4−6 nm) is very small compared to the thickness of silica film (150−160 nm). A bright thin film in the tube corresponds to the gold layer, whereas thick black color represent the silica layer. The number of rolls can be calculated by the number of either gold or silica layers. Three different kinds of silica/gold hybrid tubes were fabricated by depositing gold layer after the PDMS layer deposition (Figure 8a), before the PDMS layer deposition (Figure 8 b), and, before and after the PDMS layer (Figure 8d). A magnified SEM image of Figure 8b is shown in Figure 8c. In the corresponding Figure 8d, one can see the double gold layer in the middle of two silica layers.

The surface chemistry of the silica and silica/gold hybrid tubes was further characterized by XPS. Figure 9 shows the XPS spectra of polymer, silica and silica/gold hybrid tube. The XPS spectra clearly revealed that the intensity of the characteristics peaks of polymer C1s was drastically reduced after the pyrolysis. The XPS spectrum of silica tube showed characteristic peak of Si 2s, Si 2p, O 1s at 154 eV, 103 and 533.5 eV, respectively. For the silica tubes the [Si]:[O] ratio was found to [Si]:[O] = 0.467, which is very closed to the stoichiometric ratio of SiO_2. The origin of the residual carbon (C 1s peak) in silica and silica/gold tubes could be explained by nonspecifically adsorbed surface contaminations, which are typical for all metal and ceramic surfaces. The characteristic signals of gold (Au $4p_{3/2}$, $4p_{1/2}$, 4s, $4d_{3/2}$, $4d_{5/2}$, $4f_{7/2}$, $4f_{5/2}$, $5p_{3/2}$, and $5p_{1/2}$) were also clearly observed in the XPS spectrum of hybrid tube (Figure 9c). Furthermore, Si and O peaks also appear at their normal binding energies but the peak intensity become very poor because the gold layer covers the silica surface in hybrid tube.

The main advantage of the approach presented here is the possibility of the formation of silica and silica/metal

(34) Camino, G.; Lomakin, S. M.; Lazzari, M. *Polymer* **2001**, *42*, 2395.

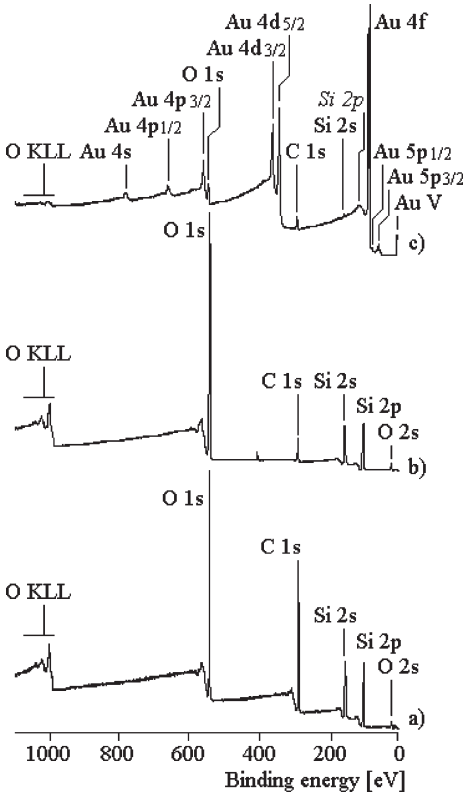

Figure 9. XPS spectra of tubes: (a) PDMS/PS/P4 VP, (b) silica tube, (c) silica/gold hybrid tube.

hybrid tubes of very high aspect ratio. The length of the tubes was limited only by the size of the substrate and of the polymer film coated on it. Microtubes as long as 2 cm were fabricated. Moreover, silica can be combined with any combination of single or multimetals resulting in hybrid tubes with a range of properties. The diameter of the tube could be tuned by changing the thickness of polymer/metal layers and the number of rolls can be controlled by time of rolling. The silica tubes with more controlled pore diameter could serve as promising host for drug delivery, whereas the silica/metal hybrid tubes could find potential application in catalysis. Furthermore, high thermal and chemical stability, photoluminescency, and biocompatibility of silica and silica/metal hybrid tubes will also result in interesting applications of these tubes in micro and nanoelectronics, optoelectronics, waveguide, and micro- and nanofludic devices.

4. Conclusions

We demonstrated a novel approach for the fabrication of silica and silica/gold hybrid tubes via self-rolling approach. Polymer tubes made from a trilayer of PDMS/P4 VP/PS were used as a precursor for such tube. The thermal decomposition of the tubes via oxidative pyrolysis led to the removal of organic moieties and the transformation of PDMS into silica. The shrinkage in the tube during the pyrolysis process led to the formation of silica tubes with pores of few hundred nanometers. The silica and silica/metal hybrid tube have potential applications in optical device (sensors, actuators), catalytic components, and tissue engineering matrices. It should be noted here that although in this study we emphasized only silica and silica/gold hybrid, this novel approach could also be used for the fabrication of other ceramic or ceramic/metal hybrid tubes.

Acknowledgment. We are grateful to Dr. Petr Formanek for his help in SEM and FIB images. We also acknowledge the help of Gudrun Adam in FTIR measurements. We thank Dr. Stefan Hoffmann, Mrs. P. Scheppan, and Dr. U. Burkhardt from Max Planck Institute of Chemical Physics of Solids, Dresden, for their help in EDX analysis. This work was financially supported by DFG (Project STA 324/41.1).

Supporting Information Available: EDX spectra of silica and silica/gold tubes; low-resolution optical microscopy image of silica tube (PDF). This material is available free of charge via the Internet at http://pubs.acs.org/.